Supplemental Appendix

Akhil Rao, Matthew Burgess, Daniel Kaffine

February 5, 2019

1 Calibrating the physical model

Our physical model uses the accounting relationships in the aggregate stocks of satellites and debris for the laws of motion, and draws on Bradley and Wein (2009) for the functional forms of the new fragment creation and collision rate functions. The scale of the time period is taken as one year, but can be shortened or lengthened by adjusting the discount rate and profits per satellite. S_t denotes the number of active satellites in an orbital shell in period t, D_t the number of debris objects in the shell in t, X_t the number of satellites launched in t, ℓ_t the probability that an active satellite in the shell will be destroyed in a collision in t, Z_t is the fraction of satellites which deorbit in t, and μ is the average amount of debris generated by deorbiting satellites. δ is the average proportion of debris objects which deorbit in t, and $G(S_t, D_t, \ell_t)$ is the number of new debris fragments generated due to all collisions between satellites and debris. m is the number of debris pieces contributed by satellites launched. A_t is the number of anti-satellite missile tests conducted in t, and γ_A is the average number of fragments created by one test. L_t is the number of satellites actually destroyed in collisions with other satellites or debris. [1]

The number of active satellites in orbit is modeled as the number of launches in the previous period plus the number of satellites which survived the previous period. The amount of debris in orbit is the amount from the previous period which did not decay, plus the number of new fragments created in collisions, plus the amount of debris in the shell created by new launches. Formally,

$$S_{t+1} = S_t - L_t - Z_t S_t + X_t \tag{1}$$

$$D_{t+1} = D_t(1-\delta) + \mu Z_t S_t + mX_t + G(S_t, D_t, \ell_t) + \gamma_A A_t. \tag{2}$$

Bradley and Wein (2009) use an ideal gas model to parameterize $G(S_t, D_t, \ell_t)$ as a quadratic function of the number of objects in orbit. We therefore approximate it as

$$G(S_t, D_t, \ell_t) = \beta_{SS}\left(\frac{S_t}{S_t + D_t}\right)\ell_t S_t + \beta_{SD}\left(\frac{D_t}{S_t + D_t}\right)\ell_t S_t + \beta_{DD}\alpha_{DD}D_t^2, \tag{3}$$

[1] For most of our sample, L_t is zero. We use ℓ_t rather than L_t in equation 2 because the p_c term in the ECOB risk index, which we use to measure ℓ_t, proxies for unobserved collisions including non-catastrophic ones. Second, as the number of objects and time horizon increase, the fraction of satellites destroyed in collisions converges to the probability an active satellite is destroyed in a collision.

where the α_{jk} parameters are intrinsic collision probabilities between objects of type j and k, and β_{jk} parameters are effective numbers of fragments from such collisions[2]. Similarly, we parameterize ℓ_t as

$$\ell_t = \alpha_{SS} S_t^2 + \alpha_{SD} S_t D_t \tag{4}$$

where the α_{SS} and α_{SD} parameters measure intrinsic probabilities of satellite-satellite and satellites-debris collisions. We refer to the intrinsic collision probabilities and effective numbers of fragments as *structural physics parameters*. Equations 2, 3, and 4 can be viewed as reduced-form statistical models which recreate the results of higher-fidelity physics-based models of debris growth and the collision rate

1.1 Data

We use data on satellites in orbit from the Space-Track dataset hosted by the Combined Space Operations Center (CSpOC) (Combined Space Operations Center, 2018) to construct the satellite stock and launch rate series. The Space-Track dataset provides details on active payloads in LEO and their decay dates. We construct the launch rate as

$$X_t = S_{t+1} - S_t + Z_t S_t + L_t, \tag{5}$$

where S_t is the number of active payloads in year t and $Z_t S_t$ is the number of payloads listed as decayed in year t.

The debris and collision risk series' we use were provided by the European Space Agency. We use debris data from the DISCOS database (European Space Agency, 2018) and collision risk data provided by Dr. Francesca Letizia (Letizia, Lemmens, and Krag, 2018) (the variable p_c in that paper). We use only objects with a semi-major axis of 2000km or less in all our data series. We prefer to use the DISCOS fragment data rather than the Space-Track fragment data as it tracks fragments from the time they were created or detected, whereas the Space-Track data tracks fragments from the time their parent body was launched. The DISCOS attribution method is closer to how economic agents in our model receive information and make decisions. We record the number of anti-satellite missile tests in a year using data from Wikipedia (**?**).

1.2 Calibration procedure

We calibrate equations 4 and 2 by estimating the following equations:

$$E_{t-1}[\ell_t | S_t, D_t] = a_{\ell 1} S_t^2 + a_{\ell 2} S_t D_t + \varepsilon_{\ell t} \tag{6}$$

$$D_{t+1} = a_{D1} D_t + a_{D2} Z_t S_t + a_{D3} X_t + a_{D4} \left(\frac{S_t}{S_t + D_t} \right) \ell_t S_t + a_{D5} \left(\frac{D_t}{S_t + D_t} \right) \ell_t S_t + \tag{7}$$

$$a_{D6} D_t^2 + a_{D7} A_t + \varepsilon_{Dt}, \tag{8}$$

[2]"Intrinsic collision probabilities" measure the probability that two objects of given sizes moving randomly in a box of fixed volume will collide in a unit of time. "Effective numbers of fragments" measure the number of new fragments weighted by the time they spend inside the volume of interest.

where ε_{xt} are mean-zero error terms to minimize and a_{xi} are parameters to estimate. All a_{xi} are nonnegative in theory, with a_{S1} and a_{D1} being in $(0,1)$. The correspondence between a_{xi} and the structural physics parameters is shown below:

$$a_{\ell 1} = \alpha_{SS}, \;\; a_{\ell 2} = \alpha_{SD}$$
$$a_{D1} = 1-\delta, \;\; a_{D2} = \mu, \;\; a_{D3} = m, \;\; a_{D4} = \beta_{SS}, \;\; a_{D5} = \beta_{SD}, \;\; a_{D6} = \beta_{DD}\alpha_{DD}, \;\; a_{D7} = \gamma_A$$

β_{DD} and α_{DD} are not separately identified from these regressions.

We estimate equation 6 using OLS on the full sample, and equation 7 using ridge regression on a quarter of the sample, evenly spaced. The fitted values are shown against the actual values with residuals in figure 1. We report a sensitivity analysis of our sampling procedure for equation 7 in the Appendix.

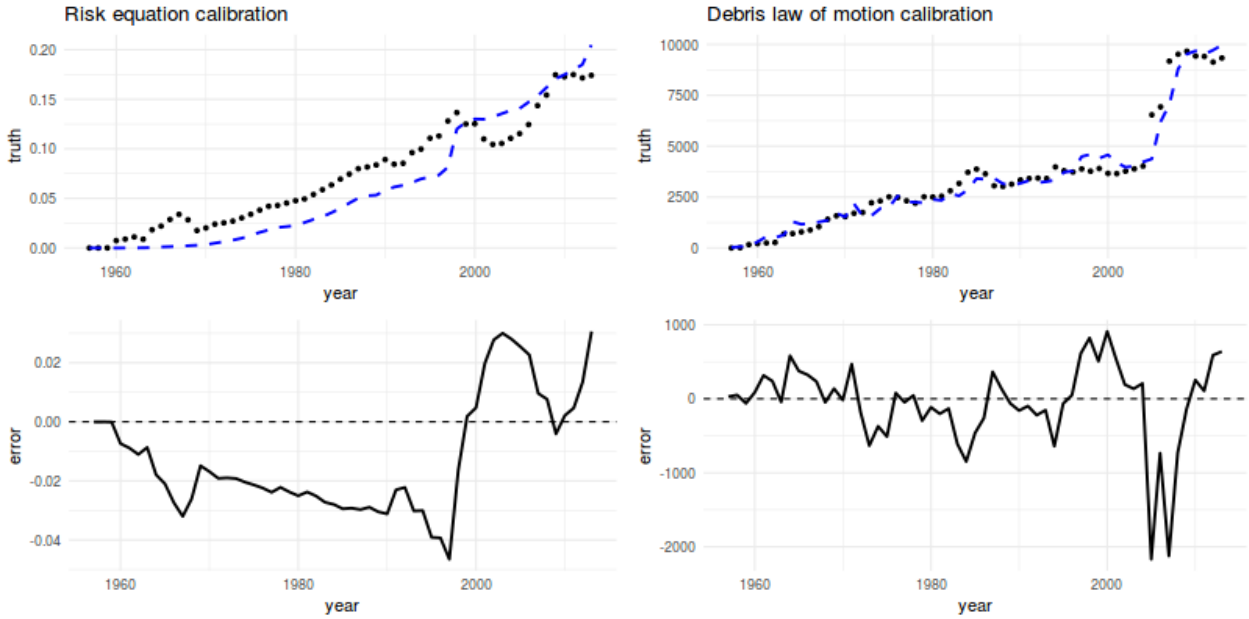

Figure 1: *Calibration fit.*
The upper panels show fitted values (blue dashed line) against actual values (black dots). The lower panels show the residuals.

Tables 1 and 2 show the calibrated parameters:

Expected collision risk parameters:	α_{SS}	α_{SD}
Parameter values:	1.15e-09	9.49e-11
Standard errors:	7.71e-11	2.2e-11

Table 1: Parameter values from estimating equation 6.

Debris law of motion parameters	δ	μ	m	γ_A	β_{SS}	β_{SD}	$\beta_{DD}\alpha_{DD}$
Parameter values:	0.52	5.83	2.19	604.04	336.42	127.96	2.1e-05

Table 2: Parameter values from estimating equation 7. All values except $\beta_{DD}\alpha_{DD}$ are rounded to two decimal places. Standard errors are not reported due to the estimation bias in ridge regression.

These parameter values are physically plausible, with the values estimated for equation 7 being lower bounds[3]. For example, the value of m suggests that every satellite launched creates 2.19 pieces of debris on average, while the value of γ_A suggests that anti-satellite missile tests create 604.04 pieces of debris on average. While the true number is likely to be higher, the orders of magnitude between γ_A, β_{SS}, and β_{SD} seem reasonable: firing a missile at a satellite creates the most debris due to the explosives involved, collisions between two satellites creates an intermediate amount of debris, and collisions between a satellite and a debris fragment create the least amount of debris in part because there is the least amount of mass to be fragmented. The expected amount of debris created by debris-debris collisions is $2e-05$ fragments - a small number, but plausible considering that fragments are small and (a) unlikely to collide, and (b) have less mass to be fragmented when they do collide.

2 Calibrating the economic model

Our economic model draws on Rao and Rondina (2018) to determine the satellite launch rate, X_t, as a function of the collision risk, ℓ_{t+1}, and the excess return on a satellite, $r_s - r$. In the simplest case, where all of the economic parameters are constant over time, the launch rate equates the conditional collision risk with the excess return:

$$E_t[\ell_{t+1}|S_{t+1}, D_{t+1}] = \underbrace{r_s - r}_{\substack{\text{excess return} \\ \text{on a satellite}}} , \tag{9}$$

where r_s is the per-period rate of return on a single satellite (π/F, where π is the per-period return generated by a satellite and F is the cost of launching a satellite, inclusive of non-launch expenditures such as satellite manufacturing and ground stations) and r is the risk-free interest rate.[4]

Equation 9 can therefore also be used to calculate the implied IRR for satellite investments from observed data on collision risk and satellite returns. r is not observed in our data. When

[3]Ridge estimates are biased toward zero relative to OLS estimates. For a given penalty parameter $\lambda \geq 0$, the relationship between a ridge coefficient estimate $\hat{\beta}^{\text{ridge}}$ and the corresponding OLS estimate $\hat{\beta}^{\text{OLS}}$ is $\hat{\beta}^{\text{ridge}} = \hat{\beta}^{\text{OLS}}/(1+\lambda)$.

[4]More precisely, r is the opportunity cost of funds invested in launching a satellite, and may diverge from the risk-free rate if the satellite launcher's most-preferred alternate investment is not a risk-free security. This rate is sometimes referred to as the internal rate of return (IRR).

costs, returns, and the discount rate are all time-varying, equation 9 becomes

$$E_t[\ell_{t+1}|S_{t+1},D_{t+1}] = 1 + r_{s,t+1} - (1+r_t)\frac{F_t}{F_{t+1}} \tag{10}$$

$$\implies E_t[\ell_{t+1}|S_{t+1},D_{t+1}] = \underbrace{\left(r_{s,t+1} - r_t\frac{F_t}{F_{t+1}}\right)}_{\substack{\text{excess return} \\ \text{on a satellite}}} + \underbrace{\left(1 - \frac{F_t}{F_{t+1}}\right)}_{\substack{\text{capital gains} \\ \text{from open access} \\ \text{and satellite launch} \\ \text{cost variation}}} \tag{11}$$

where $r_{s,t+1} = \pi_{t+1}/F_{t+1}$. With time-varying economic parameters, two sources of returns drive the collision risk. One is the excess return realized in $t+1$ from launching a satellite in t. The other is the capital gain (or loss) due to open access and the change in satellite costs. Since open access drives the value of a satellite down to the total cost of launching and operating it, F_t becomes the cost of receiving F_{t+1} in present value the following period, and the returns are given as percentages of F_{t+1}.

2.1 Data

We use data on satellite industry revenues from Wienzierl (2018), and data on satellites in LEO (semi-major axis less than 2000km) from the Union of Concerned Scientists' list of active satellites (Union of Concerned Scientists, 2018). The economic data provide a breakdown of revenues across satellite manufacture, launch, insurance, and products and services. The satellite industry revenues data cover 2005-2015, while the active satellites data cover 1958-2017.

We calculate the per-period returns on owning a satellite (π_t) as the revenues generated from commercial space products and services, and the per-period costs of launching a satellite (F_t) as the sum of revenues from commercial infrastructure and support industries, ground stations and equipment, commercial satellite manufacturing, and commercial satellite launching. The ratio π_t/F_t then gives a time series of the rate of return on a single satellite, as the number of satellites cancels out of the numerator and denominator. Since the numbers provided in Wienzierl (2018) are for the satellite industry as a whole, the ratio still needs to be adjusted to represent satellites in LEO. We do not explicitly conduct this adjustment, but let the adjustment be calculated during the estimation of equation 10.[5]

2.2 Calibration procedure

Since r is unobserved, we calibrate equation 10 by estimating

$$E_{t-1}[\ell_t|S_t,D_t] = a_{\ell 1} + a_{\ell 2}r_{st} + a_{\ell 3}\frac{F_{t-1}}{F_t} + \varepsilon_{rt}, \tag{12}$$

[5]Another way to perform this adjustment is by calculating the yearly share of satellites in LEO and multiplying the ratio π_t/F_t by the share in LEO. This approach is difficult to generalize to future years, and runs the risk of "data-snooping": since we are trying to predict the launch rate using only economic parameters (returns, costs, interest rates), incorporating the share of satellites in LEO adds physical information to the economic estimation.

using OLS on the full sample[6], where ε_{rt} is a mean-zero error term, $a_{\ell 2}$ is a scale parameter, and $a_{\ell 3}$ measures the gross IRR, $1+r$. The fitted values are shown against the actual values with residuals in figure 2.[7]

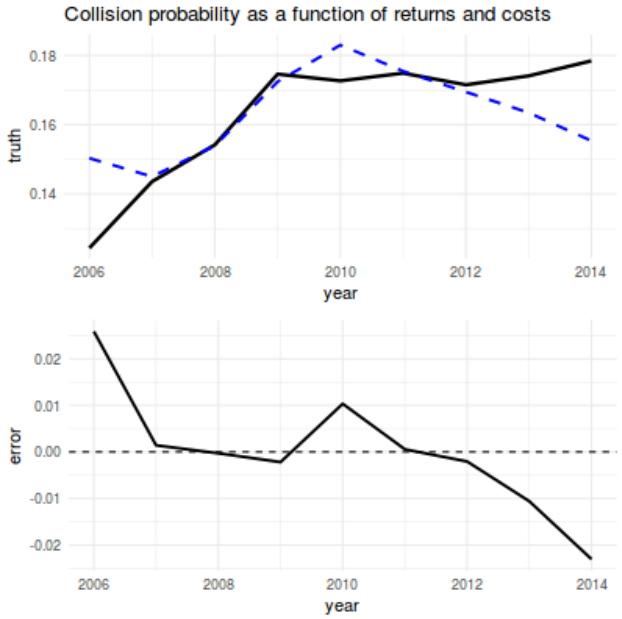

Figure 2: *Calibration fit.*
The upper panel shows fitted values (blue dashed line) against actual values (black solid line). The lower panel shows the residuals.

Tables 3 shows the calibrated parameters:

Economic calibration parameters:	$a_{\ell 1}$	$a_{\ell 2}$	$a_{\ell 3}$
Parameter values:	0.004	0.009	- 0.0004
Standard errors:	0.002	0.002	0.001

Table 3: Parameter values from estimating equation 10. All values are rounded to the first non-zero digit.

If our data perfectly measured the costs and returns of satellite ownership, and our theoretical model held exactly, we would expect $a_{\ell 1} = 1$, $a_{\ell 2} = 1$, and $a_{\ell 3} < -1$. Instead, we estimate $a_{\ell 1} = 0.004$, $a_{\ell 2} = 0.009$, and $a_{\ell 3} = -0.0004$. This suggests that our returns and cost series are measured with error or that our theoretical model is missing some important factors, such as constraints on the number of launches possible each period. These are discussed in 4.2 in the Appendix.

[6]We omit the first observation, for 2005, to construct F_{t-1}/F_t.

[7]While the theoretical model prescribes that $E_{t-1}[\ell_t|S_t,D_t]$ is the object being controlled by the period $t-1$ launch rate, we use the observed ℓ_t as a stand-in for $E_{t-1}[\ell_t|S_t,D_t]$. This is consistent with satellite launchers holding rational expectations over the future state of the orbit. While rational expectations may not be exactly true of such agents, given the planning and resources required to implement capital-intensive projects such as satellite construction and launch, we believe it to be a reasonable approximation.

Year	Observed return	Observed cost	Implied cost
2006	70.44	161.02	194.26
2007	73.87	185.5	305.31
2008	85.5	170	267.32
2009	93.06	137.81	225.56
2010	101.51	136.16	249
2011	108.84	166.99	264.08
2012	114.55	186.88	295.66
2013	120.25	215.9	301.63
2014	123.18	254.39	299.59

Table 4: Launch costs implied by open access and observed values. All values are given in billions of nominal US dollars per year.

Regardless of the factors missing from the theoretical model, we use equation 12 to recursively calculate the sequence of launch costs implied by the combination of open access, observed launch rates, and observed satellite returns as

$$\begin{aligned} E_{t-1}[\ell_t|S_t,D_t] &= a_{\ell 1} + a_{\ell 2} r_{st} + a_{\ell 3}\frac{F_{t-1}}{F_t} + \varepsilon_{rt} \\ \implies \hat{F}_t &= \frac{a_2\pi_t + a_3 F_{t-1}}{\ell_t - a_1}. \end{aligned} \tag{13}$$

Table 4 shows the observed satellite returns (π_t), observed launch costs (F_t), and implied launch costs ($\hat{F}_t$).

3 Computing satellite tax projections

With the calibrated parameter values, we turn to computing satellite tax projections. We split this process into two stages. First, we compute open access and optimal launch policy functions in each period using the calibrated parameter values. These functions prescribe the number of satellites launched under each type of management regime for a given level of satellite and debris stocks. Then, we use an interpolation scheme (described in section 4.3 of the Appendix) to generate launch rate predictions from the policy functions and observed orbital stocks at the start of the forecast period. We show the in-sample fit of our open access projections to establish that our approach can approximate the observed history, and then use predictions of space economy revenues and costs from [ADD CITE – MORGANSTANLEY] to project out the open access and optimal launch rates given those predictions. We calculate the optimal satellite tax along those time paths using the relation described in equation 14 below:

$$\tau_t = (E_t[\ell_{t+1}|\hat{S}_{t+1},\hat{D}_{t+1}] - E_t[\ell_{t+1}|S^*_{t+1},D^*_{t+1}])F_{t+1}, \tag{14}$$

where $\hat{S}_{t+1}$ and $\hat{D}_{t+1}$ are satellite and debris stocks in $t+1$ under open access management, and S^*_{t+1} and D^*_{t+1} are satellite and debris stocks in $t+1$ under optimal management. This formula is drawn from Rao and Rondina (2018), and the optimal tax is positive as long as the planner would

maintain lower collision risk than firms under open access would. Intuitively, since firms under open access set the collision risk equal to the excess return on a satellite while the planner sets the collision risk equal to the excess return of a satellite minus its marginal external cost, the difference in these collision risks gives us the marginal external cost of a satellite. By charging open access firms the marginal external cost of their satellite as a tax, their incentives are aligned with those of the planner despite the difference in legal institutions.

3.1 Open access and optimal policy functions

We generate two sequences of policy functions: one function for each period under consideration, and one sequence for each management regime type. We compute each sequence through backwards induction: beginning at the final period in our projection horizon, and iteratively working backwards to the initial period. This procedure implies "perfect foresight" planning under each management regime, i.e. that all agents under any management regime are able to perfectly forecast the sequence of returns, costs, interest rates, launch rates, and other model objects. The perfect foresight assumption is clearly unrealistic, but our purpose is not to show how uncertainty in economic parameters propagates over time. Rather, our purpose is to show how an optimal satellite tax would vary over time and the time paths of orbital aggregate stocks under different management regimes. Such assumptions are used in integrated assessment models of climate change with similar rationales [ADD CITE – IAMs AND PERFECT FORESIGHT]. Our work here is conceptually similar to climate IAMs.

To compute the open access time path, we first generate a grid of satellite and debris levels, $(grid_S, grid_D)$. We generate this grid as an expanded Chebyshev grid to reduce numerical errors from interpolation, provide higher fidelity near boundaries, and economize on overall computation time. In contrast to a standard Chebyshev grid, an expanded Chebyshev grid allows for computation (rather than extrapolation) at the boundary points. The formula for the k^{th} expanded Chebyshev node on an interval $[a,b]$ with n points is

$$x_k = \frac{1}{2}(a+b) + \frac{1}{2}(b-a)\sec\left(\frac{\pi}{2n}\right)\cos\left(\frac{k}{n} - \frac{1}{2n}\right)$$

We set $a = 0$ and $b = 25000$ for both S and D, creating a square grid. The main issue in setting b is ensuring that the time paths we solve for (described in the next section) do not run into or beyond the boundary.

In general, computing decentralized solutions under open access is simpler than computing the planner's solutions. This is because open access simplifies the continuation value to the cost of launching a satellite. We use `R` for all simulations, parallelizing where possible.

We compute optimal value functions by alternating between value function iteration and policy evaluation on a grid of the state variables S and D. We initialize the algorithm with a guess of the value and policy functions. Algorithm 1 describes how we compute the optimal policy and value functions for a given grid and given value function guess $guess(S,D)$, while algorithm 2 describes how we compute the open access policy and value functions on the same grid.

We construct our initial guess of the planner's value function as the terminal value of the fleet. In the penultimate period, we assume it is not optimal to launch any satellites ($X^*_{T-1} = 0$), making the final fleet size

$$S_T = S_{T-1}(1 - E_{T-1}[\ell_T | S_{T-1}, D_{T-1}]).$$

In the final period (T), the payoff of the fleet is πS_T. Our assumption that it is not optimal to launch any satellites in the penultimate period implies that the one-period returns of a satellite do not cover the cost of building and launching ($\beta \pi_T < F_{T-1}$), which we verify to hold in every period of our data.

To construct the implied series of F_t given the observed π_t and launch rate series', we solve equation 10 using the estimated coefficients from equation 12. We denote the implied launch cost as $\hat{F}_t$ and the implied rate of return on a satellite as $\hat{r}_{st}$. We use these values in solving for open access and optimal policies.

Algorithm 1: Value function iteration with policy evaluation

Set

$$W_0(S,D) = guess(S,D),$$
$$X_0 \equiv 0$$

for all $(S,D) \in (grid_S, grid_D)$

Set $i = 1$ and $\delta = 100$ *(some large initial value).*

while $\delta > \varepsilon$ **do**

At each grid point in $(grid_S, grid_D)$, use a numerical global optimizer to obtain

$$X_i = \text{argmax}_X\{\pi S - \hat{F}X + \beta \hat{W}_{i-1}(S',D')\},$$
$$W_i(S,D) = \pi S - FX_i + \beta \hat{W}_{i-1}(S',D'),$$

where $\hat{W}_{i-1}(S',D')$ is computed by linear interpolation from $W_{i-1}(S,D)$, $S' = S(1-\ell) + X_i$, $D' = D(1-\delta) + G(S,D,\ell) + mX_i$, and $\ell = \min\{a_{\ell 1}S^2 + a_{\ell 2}SD, 1\}$.

$\delta \leftarrow ||W_i(S,D) - W_{i-1}(S,D)||_\infty$.

$\delta_{policy} \leftarrow ||X_i^* - X_{i-1}||_\infty$

if $\delta_{policy} < 1$ *(some fixed small value),* **then**

Evaluate the policy. Compute $W_i^T(S,D) = \sum_{t=1}^{T-1} \beta^{t-1}(\pi S_t - \hat{F}X_t^*) + W_i(S_{t+1}, D_{t+1})$ by backwards induction, using the laws of motion for S_{t+1} and D_{t+1} and the form of $E[\ell_{t+1}|S_{t+1}, D_{t+1}]$. We use progressively increasing values of T, beginning at 2 and rising with i to a maximum of 75. Set $W_i(S,D) = W_i^T(S,D)$ and return to step (a).

end

i ← i+1

end

Algorithm 2: Open access launch plan computation

Use a numerical rootfinder to find the X_{t-1}^o which solves

$$\ell_t = a_{\ell 1} + a_{\ell 2}\hat{r}_{st} + a_{\ell 3}\frac{\hat{F}_{t-1}}{\hat{F}_t},$$

where $\ell_t = \min\{a_{\ell 1}S_t^2 + a_{\ell 2}S_tD_t, 1\}$, and $S_t = S_{t-1}(1-\ell_{t-1}) + X_{t-1}$, $D_t = D_{t-1}(1-\delta) + G(S_{t-1}, D_{t-1}, \ell_{t-1}) + mX_{t-1}$.

Approximate $W_i^\infty(S,D) = \sum_{t=1}^\infty \beta^{t-1}(\pi S_t - \hat{F}X_t^o)$ as $W_i^T(S,D) = \sum_{t=1}^{T-1} \beta^{t-1}(\pi S_t - \hat{F}X_t^*)$ by backwards induction, using the laws of motion for S_{t+1} and D_{t+1} and $\ell_t = \min\{a_{\ell 1}S_t^2 + a_{\ell 2}S_tD_t, 1\}$. We use $T = 500$.

3.2 Generating time paths

We use algorithms 1 and 2 to compute policy and value functions in each period, and run them sequentially from the final period to the first period to generate a series of policy and value functions for each period's set of economic parameters. Algorithm 3 describes this process.

Algorithm 3: Generating a perfect-foresight sequence of policy functions

1 Set economic parameters to final period values.
2 Run Algorithm 1 (for an optimal path) or 2 (for an open access path).
3 **for** *t in T-1:1* **do**
4 Using the value function from the previous step as $W(S_{t+1}, D_{t+1})$, calculate

$$X^* = \text{argmax}_X\{\pi_t S - \hat{F}_t X + W(S_{t+1}, D_{t+1})\} \quad \text{(for an optimal path)}$$

or

$$X^o : \ell_t = a_{\ell 1} + a_{\ell 2}\hat{r}_{st} + a_{\ell 3}\frac{\hat{F}_{t-1}}{\hat{F}_t} \quad \text{(for an open access path),}$$

using the laws of motion for S_{t+1} and D_{t+1} and $\ell_t = \min\{a_{\ell 1}S_t^2 + a_{\ell 2}S_t D_t, 1\}$, linearly interpolating $W(S_{t+1}, D_{t+1})$.
5 If calculating an optimal path, set $W(S_t, D_t) = \pi_t S - \hat{F}_t X^* + W(S^*_{t+1}, D^*_{t+1})$. If calculating an open access path, set $W(S_t, D_t) = \pi_t S - \hat{F}_t X^o + W(S^o_{t+1}, D^o_{t+1})$.
6 **end**

It is important to note that when obtaining the sequence of policy functions we do not do backwards induction within each economic time period prior to the final period. Instead, we hold the continuation value fixed, and iterate on the policy functions, using previous iterations as starting points. This ensures that the continuation value incorporates each period's returns and costs only once until the final period. Backwards induction on the value function in the final period treats that period's costs and returns as steady state values.

Once we have a sequence of policy functions for each period's economic parameters, we generate time paths by picking a starting condition (S_0, D_0), computing the launch rate X_0 by thin-plate spline interpolation of the policy function, using the launch rate to compute the next-period state variables, and repeating the process until the terminal period. Figure 3 shows the simulated open access and optimal paths of launches, satellites, debris, and collision risk. Figure 4 shows the paths of the flow of instantaneous welfare gains from open access (interpretable as the incentive to private agents to avoid self-regulation), the net present value of welfare losses from open access (the capitalized benefit to society from optimal orbit management), the price of anarchy under open access (the ratio of open access collision risk to optimal risk), and the path of an optimal satellite tax beginning in 2005.

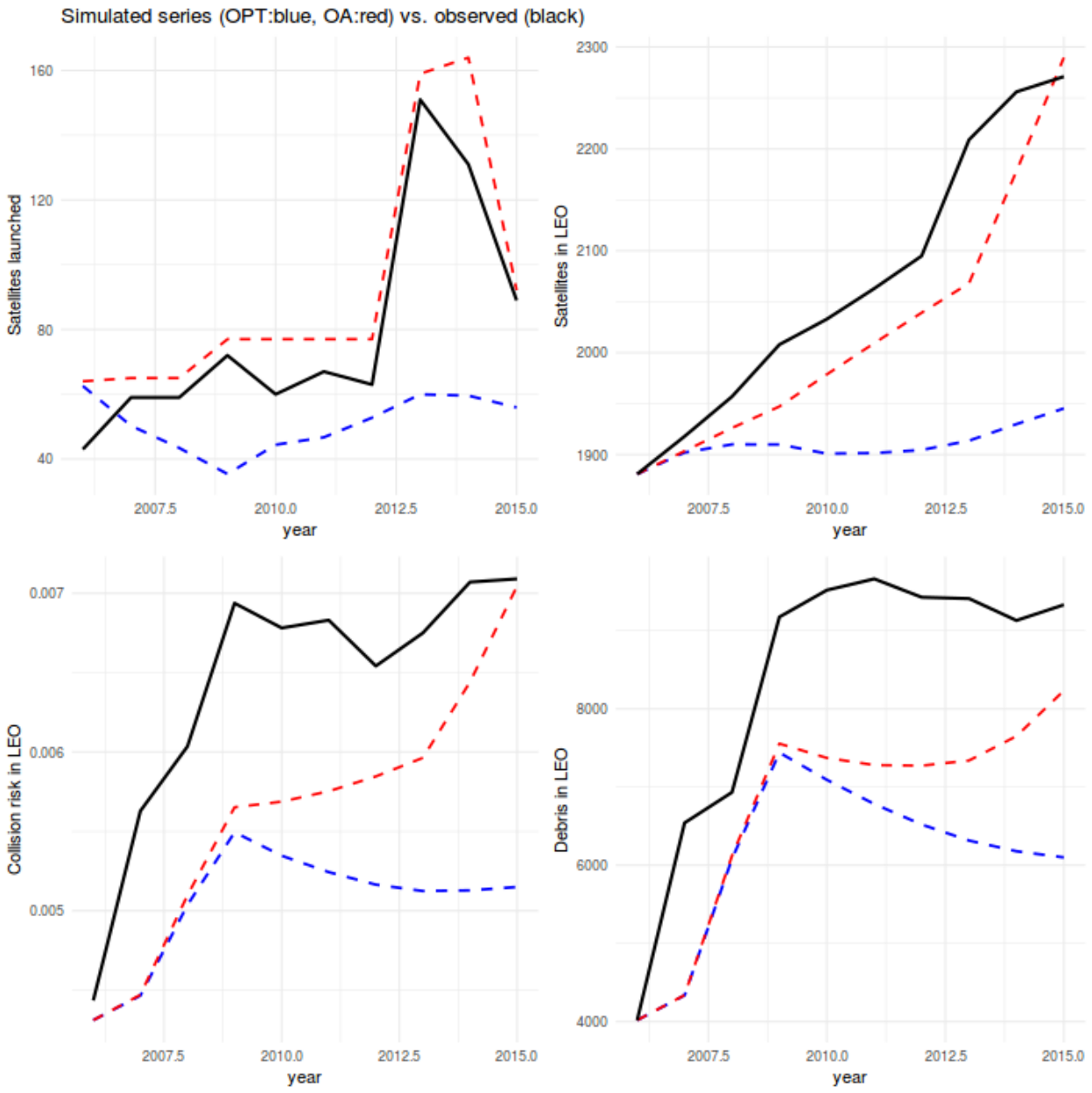

Figure 3: *Projected time paths of orbital aggregates.*
The red lines show simulated open access paths. The blue lines show simulated optimal paths. The black lines show observed time paths (where data are available).

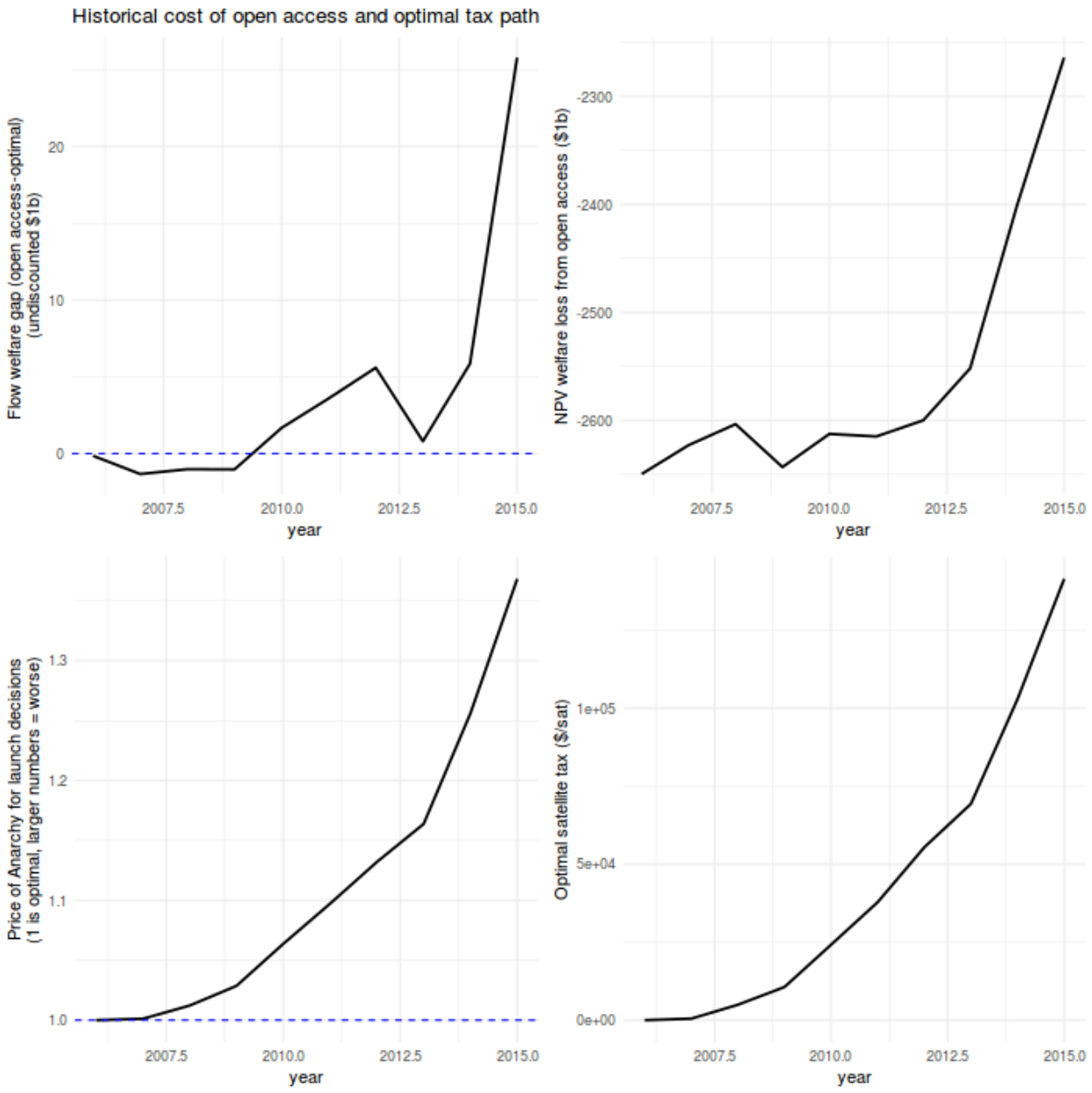

Figure 4: *Projected time paths of private gains, social losses, degree of suboptimal risk, and optimal satellite tax.* From the upper left, going clockwise: the flow of instantaneous welfare gains from open access (the incentive to private agents to avoid self-regulation), the net present value of welfare losses from open access (the capitalized benefit to society from optimal orbit management), the path of an optimal satellite tax beginning in 2005, and the price of anarchy under open access (the degree to which open access risk exceeds optimal risk).

References

Bradley, Andrew M. and Lawrence M. Wein. 2009. "Space debris: Assessing risk and responsibility." *Advances in Space Research* 43:1372–1390.

Combined Space Operations Center. 2018. "Space-Track.org Satellite Catalog." From Space-Track.org at `https://www.space-track.org/`.

European Space Agency. 2018. "DISCOS database." From ESA at `https://discosweb.esoc.esa.int/web/guest/home`.

Letizia, F., S. Lemmens, and H. Krag. 2018. "Application of a debris index for global evaluation of mitigation strategies." 69th International Astronautical Congress.

Rao, Akhil. 2018. "Economic Principles of Space Traffic Control." Latest draft available at `https://akhilrao.github.io/assets/working_papers/Econ_Space_Traffic_Control.pdf`.

Rao, Akhil and Giacomo Rondina. 2018. "Cost in Space: Debris and Collision Risk in the Orbital Commons." Latest draft available at `https://akhilrao.github.io/assets/working_papers/Cost_in_Space.pdf`.

Union of Concerned Scientists. 2018. "UCS Satellite Database." From UCS at `https://www.ucsusa.org/nuclear-weapons/space-weapons/satellite-database`.

Wienzierl, Matthew. 2018. "Space, the Final Economic Frontier." *Journal of Economic Perspectives* 32:173–192.

4 Appendix

4.1 Sensitivity analysis of sampling procedure for estimating equation 7

We estimate equation 7 using only a quarter of the sample to avoid overfitting. To evaluate how sensitive the predictions and coefficient estimates are to our sampling procedure, we conduct a sensitivity analysis. Our procedure is straightforward. We randomly draw a quarter of the sample (15 observations) 1000 times, estimate equation 7 on each random sample, and plot the predictions against the observed D_{t+1} in figure 5. We also take the mean of the estimated coefficients and compare them against the model we selected in table 2. Table 5 shows the comparison.

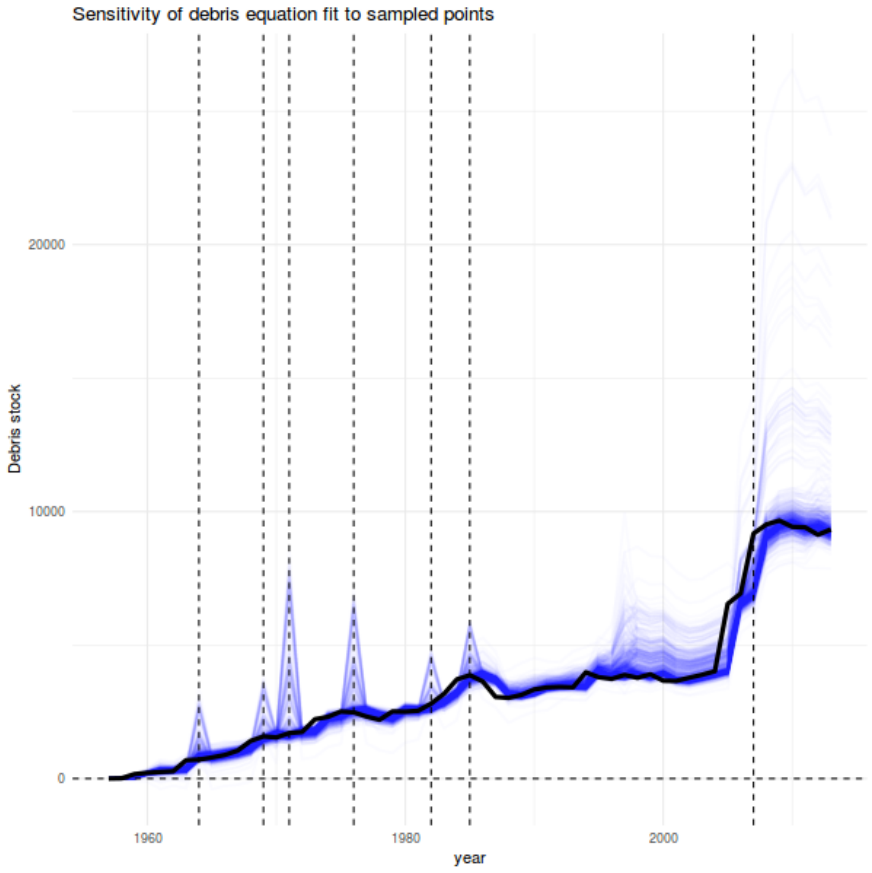

Figure 5: *Calibration fit.*
The thin blue lines show fits from random samples. The thick black line shows the actual debris time series. The large sometimes-negative spikes in the predicted series' correspond to anti-satellite missile tests, of which the 2007 FY-1C test generated the most debris.

Debris law of motion parameters	δ	μ	m	γ_A	β_{SS}	β_{SD}	$\beta_{DD}\alpha_{DD}$	λ
Model selected in table 2:	0.52	5.83	2.19	604.04	336.42	127.96	2.1e-05	287.21
Mean parameter values:	0.76	16.19	2.31	156.57	487.68	137.94	1.9e-05	325.61

Table 5: Parameter values from estimating equation 7. All values except $\beta_{DD}\alpha_{DD}$ are rounded to two decimal places. λ is the ridge penalty parameter, with larger values corresponding to greater shrinkage (and coefficient bias). We selected λ by cross-validation on the training sample in all cases.

4.2 Factors which may cause coefficient attenuation

Measurement error

Random measurement error would attenuate coefficient estimates, which may partially explain why our estimated coefficients are close to zero. Non-random measurement error is another possibility.

We construct the returns and costs of satellite ownership from the data described in Wienzierl (2018), which aggregate revenues from all commercial satellites in orbit. Our physical model is based on data for low Earth orbit. To adjust the returns and costs to reflect only satellites in LEO, we multiply the per-period returns and cost series' by the share of satellites launched each year to LEO. If the returns to LEO satellites are lower than the returns to GEO satellites, then our attribution procedure would overstate the returns to LEO. The near-zero coefficients may therefore partially reflect systematically overstated returns to LEO in our constructed series'.

Launch constraints

Our theoretical model assumes that any firm which wants to launch a satellite can do so. If launches are limited, firms will be unable to do so. This will prevent open access launching from equating the excess return on a satellite with the risk of its destruction. Firms which are able to launch will then earn rents from having a satellite while the collision risk is below the excess return. The wedge between the collision risk and excess return will reflect the value of those rents.

Launch limitations which allow only $\bar{X}_t$ firms to launch in t are a type of "flow control", studied in more depth in Rao (2018). In particular, Rao (2018) establishes that flow controls which restrict the quantity of launches in each period are equivalent to flow controls which impose an additional positive price p_t on launching in t. Generalizing the flow-controlled equilibrium condition from that paper, we obtain the open access equilibrium condition for launches when costs, returns, and discount rates are all time-varying:

$$E_t[\ell_{t+1}|S_{t+1},D_{t+1}] = (1-\frac{p_t}{F_{t+1}+p_{t+1}})+\frac{\pi_{t+1}}{F_{t+1}+p_{t+1}}-(1+r_t)\frac{F_t}{F_{t+1}+p_{t+1}}, \tag{15}$$

p_t can be interpreted in two ways. It may be viewed as the implied rent received by a firm which already owns a satellite in t due to launches in t being restricted. It may also be viewed as the implied launch tax paid by a firm which is allotted a launch slot in t. In either view, a binding launch constraint results in positive values of p_t and p_{t+1}, biasing the coefficients from regression 10 downwards.

4.3 Interpolation scheme for launch time paths